J. Chem. Sci. (2019)131:104
https://doi.org/10.1007/s12039-019-1684-8

© Indian Academy of Sciences

REGULAR ARTICLE

Conversion of methanol to aromatics over ZSM-5/11 intergrowth Zeolites and bimetallic Zn-Cu-ZSM-5/11 and Ga-Ag-ZSM-5/11 catalysts prepared with direct synthesis method

MARYAM JUYBAR*, MOHAMMADREZA KANMOHAMMADI KHORRAMI and AMIR BAGHERI GARMARUDI

Chemistry Department, Faculty of Science, Imam Khomeini International University, P.O. Box 3414896818, Qazvin, Iran
E-mail: maryamjuybar.gu@gmail.com

MS received 3 April 2019; revised 15 June 2019; accepted 23 July 2019

Abstract. Catalytic conversion of methanol to gasoline range hydrocarbons, especially aromatics was carried out in a fixed bed reactor over nano-crystal composite H-ZSM-5/11 zeolite synthesized by hydrothermal method. The metals of Zn, Cu, Ga and Ag as bimetallic Zn-Cu and Ga-Ag with different concentrations (3: 2, 5: 3) and (1:1, 3:2) respectively were selected for loading into the prepared zeolite catalysts. Direct synthesis method was used for incorporating metals. Prepared zeolites were characterized by XRD, SEM, TEM, N_2 adsorption-desorption, ICP-OES, NH_3-TPD and FT-IR. After incorporation of metal species into the zeolites framework, the particles crystalline size was reduced, the intercrystalline porosity was increased, causing the formation of new moderate acid sites. The catalytic results illustrated that the incorporation of metal species enhanced the activity and catalyst stability in MTA reaction. BTX yield in ZSM-5/11 reached up at 23.5% to 30.4% and 25.88% with Zn-Cu-ZSM-5/11(1) and Ga-Ag-ZSM-5/11(1), respectively whereas heavier aromatics production reduced. Also, the comparison of catalysts with different metals content showed that due to improvement in structure and properties, low metal content zeolites have better performance in converting methanol to aromatics.

Keywords. Aromatization; BTX selectivity; Direct synthesis procedure; Bimetallic incorporation; Intergrowth structure.

1. Introduction

There is clear evidence indicating that oil reserves will not be able to supply the world's energy demand. The total fuel consumption is about 116 million tons per day, which is increasing at a growth rate of more than 3%. With this consumption rate in 2020, it will reach about 162 million tons per day.[1] Recently, methanol to gasoline (MTG) conversion has been considered as a non-petrochemical route.[2,3] Methanol is readily available from various carbon sources such as charcoal, natural gas and biomass. This process was initially used by Oil Research Group at the laboratory of Mobil Company during 1970s. In 1982, the production of aromatics, light olefins and gasoline from methanol was investigated using an acidic zeolite catalyst.[4]

Many researchers have used ZSM-5 zeolite possessing MFI type structure with medium-sized pores widely in commercial processes, especially in petroleum and petrochemical industries.[5,6] This zeolite has a 3D framework including two intersecting systems of direct channels (0.51 nm × 55 nm) and zigzag channels (0.53 nm × 0.56 nm). These interconnected channels provide a specific structure for this catalyst, with a good volume of cyclization reactions and conversion olefins to alkanes and aromatics.[7]

Commonly used zeolites are single zeolite framework-type materials. But in some cases, a combination of different zeolite structures is preferable because of specific performance. Recently, mesoporous and microporous composites such as MCM-41/ZSM-5,[8] ZSM-22/ZSM-23,[9] and ZSM-5/MCM-48[10] have been used in the catalytic applications, as they can combine the advantages of microporous materials with the large size of the pores in the mesoporous materials.

ZSM-5/ZSM-11 has been synthesized by Kokotailo as a composite zeolite for the first time.[11] This hybrid

*For correspondence

Published online: 01 November 2019

has been used to convert methanol to hydrocarbons, aromatics alkylation, isomerization and cracking processes.[12,13] ZSM-11 is a zeolite with MEL type structure. This zeolite, with the only difference being the existence of two series of intersecting straight channels, (0.53 nm × 0.54 nm) has a high structural similarity to ZSM-5 zeolite.[14,15] The diameter of the pore between MFI structure in the ZSM-5 and MEL in the ZSM-11 is approximately equal and the formation of intergrowth structure is possible between two zeolites. Based on the crystallographic analysis, the intergrowth structure effects on the size of unit cells; hence, the size and shape of the pores are changed in the straight direction.[16] Increasing the size of the pores in this structure makes a high impact on the catalytic properties based on shape-selective.

Proper adjustment of zeolite properties was achieved by using various cations replacing some zeolite framework sites. This replacement simultaneously caused certain changes in the properties of zeolites such as thermal stability, pore size and catalytic activity. Over the last few years, metals and oxides of various metals such as Fe,[17] Mo,[18] Cu,[19] Pt,[20] Gd,[21] Ni,[22] Zn,[23] Ga[24] and La[25] have been used for improved catalytic performance in the framework of zeolite.

Among the metals, Zn and Ga are the most effective metals in enhancing the aromatization of methanol and light alkanes. Zn is often formed as ZnO and $ZnOH^+$ in the framework of zeolites. $ZnOH^+$ enhance dehydrogenation of light hydrocarbons, converts them into aromatics and stops the hydrogen transfer reaction.[26] Also, the placement of gallium in zeolite ZSM-5 not only does not reduce the strength of acidic sites but also because of the creation of gallium species outside the network, has led to the formation of stronger Lewis sites that can increase the dehydrogenation step in the aromatization of olefins.[27,28]

Scurrell *et al.,* performed a comparative study of the aromatization from n-hexane with the Ga, Mo and Zn modified H-ZSM-5 catalysts. They observed that the formation of aromatics with gallium, zinc substituted catalysts due to the dehydrogenation activity of these two metals increased. But the addition of molybdenum to H-ZSM-5 increased the cracking activity and led to the production of fewer aromatics.[29]

The catalytic activity would be promoted more effectively in the presence of a second metal such as Cu, Fe, Ti, Ag and La.[30–34] The role of some of these metals has not yet been clear. It seems that CuO and ZnO loading in ZSM-5 plays an efficient role in the methanol-to-gasoline conversion. Adding CuO to HZSM-5 creates new acidic sites and increases selectivity to gasoline products while adding ZnO to this catalyst increases its stability. It also provides a better distribution of CuO particles by reducing the crystallite size. Thereby, more CuO sites are available for methanol adsorption and the catalyst activity increases.[35]

In the present work, ZSM-5/11 and bimetallic incorporated ZSM-5/11 with various loading contents of Zn – Cu (3:2, 5:3 wt%) and Ga–Ag (1:1, 3: 2 wt%) were synthesized. We study the conversion of methanol to aromatics over prepared catalysts. Metals were incorporated into the zeolites framework by direct synthesis method. The influence of metals substituted was investigated using several physicochemical technologies to demonstrate the effect of mesoporosity and acidity on the distribution of liquid products, particularly BTX and lifetime.

2. Experimental

2.1 *Material and methods*

In this synthesis, colloidal silica (Merck (Germany), 30 wt%) and sodium aluminate (Fisher (U.S.A)) were selected as silica and aluminum sources. Sodium hydroxide (Merck (Germany)) and tetra-butyl ammonium hydroxide (1M in methanol, Merck (Germany)) and deionized water were utilized for the synthesis of ZSM-5/11 zeolite. To modify the zeolite, ZnO, Cu $(NO_3)_2$. 3 H_2O, Ga $(NO_3)_3$ .xH_2O, $AgNO_3$. 3H_2O (Merck (Germany)) were used.

2.1a *Synthesis of composite ZSM-5/11 zeolite*: According to the typical synthesis procedure[36] in the synthesis of ZSM-5/11 zeolite, a clear solution with molar composition 12 N_2O: 1.0 Al_2O_3: x XO (X= Zn-Cu, Ga-Ag): 60SiO_2: 1.5 (TBA) $_2$O: 1200 H_2O was obtained.

In this process, 0.125 g of sodium aluminate and 0.54 g of NaOH were added to 12 mL of stirring distilled water. After the solution was clear, 1.35 g of tetra-butyl ammonium hydroxide and 12 mL of colloidal silica were added dropwise to it, under vigorous stirring. Fabricated white gel remained at room temperature for 24 h. Then it was transferred to an autoclave with a Teflon interior wall, being stored at 170 °C for 72 h without stirring. The sample was cooled at room temperature and washed with distilled water (3 times). The remaining solid was dried at 120 °C for 16 h and then calcinated at 550 °C for 6 h (temperature increased by 20 °C min^{-1} rate). In order to obtain acidic zeolite (HZSM-5/11), the sample was also stirred with 16.5 mL/g of 1M ammonium nitrate at 135 °C for 2 h, being cooled and washed with distilled water. This step was repeated three times. In the final step, it was calcinated at 550 °C for 4 h (temperature increased by 20 °C min^{-1} rate).

2.1b *Synthesis of metal incorporated ZSM-5/11*: Direct synthesis method was used for loading Zn-Cu and Ga-Ag into the framework of ZSM-5/11 zeolite. After

adding colloidal silica to the gel in the synthesis step, ZnO, Cu $(NO_3)_2$. $3H_2O$ and Ga $(NO_3)_3.xH_2O$, $AgNO_3$. $3H_2O$ were added to this mixture. All subsequent steps were repeated like ZSM-5 / 11 synthesis. Synthetized composite zeolites were named Zn-Cu-ZSM-5/11(1), Zn-Cu-ZSM-5/11(2) with metal content 3:2, 5:3 and Ga-Ag-ZSM-5/11(1), Ga-Ag-ZSM-5/11(2) with metal content 1:1, 3:2. According to previous studies, due to the large size of Ga-Ag particles, a smaller amount of these metals was used for loading than Zn-Cu.[37] Metal loaded content in zeolites was determined by the ICP-OES method that is represented in the first and second columns of Table 1.

2.2 *Catalyst characterization*

X-ray powder diffractometer (XRD) was used to evaluate the crystallinity, structure and purity of synthetic products. All the prepared samples were analyzed at room temperature by XRD using Philips PW 1730 Advance X-ray diffractometer (Netherlands) at 2θ range from 2° to 50° with monochromatic Cu Kα radiation (wavelength λ = 1.5406Å) under the instrumental setting of 40 kV and 40 mA. The relative crystallinity was estimated from the intensity of (051) peak at 2θ = 23° and 2θ = 7.9° revealed to the crystalline size and was calculated from Debye-Scherer equation.

$$D = {}^{0.9\lambda}/_{\beta \cos \theta}$$

D is the crystalline size (A°), λ is X-ray wavelength (1.54 A°), β is the full width at half maxima of the peaks at 2θ of 7.91, 8.81(FWHM), θ is the Bragg angle.

Elemental analysis was performed by ESPECTRO ARCOS inductively coupled plasma optical emission spectrometry (ICP-OES) analyzer to representing the amount of metal loading in the zeolite framework.

A surface-measuring device (Belsorp mini II BEL instrument (Japan)) was used to determine the specific surface area (S_{BET}) and the volume pores of zeolites. S_{BET} and micropore volume were obtained from the Brunauer-Emmett-Teller (BET) equation and the t-plot method. Mesoporous volume was determined by BJH method. Total pore volume was the volume of nitrogen absorbed at p/p_0=0.99. A density functional theory (DFT) was used to determine the particle size distribution (PSD).

TESCAN (MIRA III) Scanning electron microscope (SEM) was used to prepare micrograph images of synthetic samples. Gold coating was used to reduce the charge effect. Transmission electron microscopy (TEM) performed on Philips EM208s 100KV.

To determine surface functional groups and the nature of coke species, Fourier Transform infrared (FTIR) analyses of the sample were obtained using a Brucker FT-IR Vertex 80 spectrometer. The spectra were recorded in the range of 400–4000 cm^{-1} and the resolution of 4 cm^{-1}.

In order to measure the surface acidity of the synthetic catalyst, temperature-programmed desorption of ammonia (NH_3-TPD) technique carried out on a Micrometrics, AutoChem 2920 II instrument (USA). At first, 0.15 g of the sample was degassed under He flow (40 mL/min) at 500 °C for 90 min at a heating rate of 10 °C min^{-1}. After cooling the catalyst to 100 °C, it was exposed to ammonia for half an hour to saturate. Then, the sample was purged with helium for 30 min at 40 mL min^{-1}. This process allowed physical and poor adsorbed NH_3 to be removed from the zeolite. Hence, the temperature was raised to 750 °C at the heating rate of 10 °C min^{-1}. The amount of desorbed ammonia from the catalyst was evaluated by a thermal conductivity detector (TCD) and recorded as a function of temperature.

The coke content of the catalysts after the catalytic performance was evaluated using thermo-gravimetric analysis (TGA) with a TG instrument (SDT Q600).

2.3 *Catalytic performance tests*

The conversion of methanol was carried out by a fixed bed stainless steel reactor with an inner diameter of 9 mm at atmospheric pressure. The catalyst particles in the reactor were kept constant by quartz particles. Before the performance test, the catalysts were pressurized, broken, and sieved between 12 and 20 mesh (850–1400 μm). 1 g from each sample was placed in the middle of the reactor. The reaction temperature was measured with a stainless steel thermocouple which was deposited on the catalyst bed. Before the test, nitrogen gas was passed through the catalyst

Table 1. Metal contents, relative crystallinity and crystallite size in prepared catalysts.

Sample	Zn (wt%)[a]	Cu (wt%)[a]	Ga(wt%)[a]	Ag(wt%)[a]	Relative crystallity (%)	Crystal size (nm)[b]
ZSM-5/11	–	–	–	–	100	40
Zn-Cu-ZSM-5/11(1)	3	1.68	–	–	99.1	27
Zn-Cu-ZSM-5/11(2)	4.87	3.21	–	–	79.4	27
Ga-Ag-ZSM-5/11(1)	–	–	1.07	1.01	90.8	32
Ga-Ag-ZSM-5/11(2)	–	–	3.13	2.16	83.0	39

[a]By ICP-OES analysis.

[b]Crystallite size estimated by Scherer's equation.

at 300 °C for 2 h to activate the catalyst sites. Methanol was injected by an HPLC pump with a weight hourly space velocity (WHSV) of 4.75 h^{-1} at 390 °C. The reaction product passed through a condenser (10 °C) to collect the organic and inorganic fractions. Finally, the organic product was analyzed using offline GC-MS (Agilent 6890 (USA)). The separation of liquid compounds was performed by a column of TRB-5MS (50 m × 200 µm × 0.25 µm).

To determine the percentage of methanol conversion, separated aqueous part include water and methanol was analyzed by a BOMEM Hartmann & Braun MB-series mid-FTIR (Canada) in the range of 950–1500 cm^{-1}. Water spectrum was considered as a background. 1 mL of the aqueous fraction obtained during the conversion of methanol to gasoline was deposited on the 45° Zn-Se trough plate. After the plate was established on the horizontal attenuated total reflector holder, the ATR-FTIR spectra were recorded in the range of 800–3000 cm^{-1} with a resolution of 4 cm^{-1}. By an external standard method, a calibration model was obtained from solutions with different methanol and water ratios. The concentration of methanol in aqueous fraction was estimated by analyzing the results with Omnic software.

Methanol conversion, organic product yield and products selectivity were obtained using the following equations (Eq. 1, 2 and 3) respectively.

$$\text{Methanol conversion } (\%) = \left(W_f - W_p\right)/\left(W_f\right) \times 100\% \quad (1)$$

Where W_f and W_p are the weight of methanol in the feed and products respectively.

$$\text{Gasoline yield } (\%) = \left(W_{org}\right)/\left(W_{org} + W_{aq}\right) \times 100\% \quad (2)$$

Where W_{org} is the weight of liquid organic products and W_{aq} is the weight of the aqueous fraction

$$\text{Product selectivity } (\%) = W_p/W_t \times 100\% \quad (3)$$

Where W_p is the weight of the product and W_t is the total weight of hydrocarbon products.

3. Results and Discussion

3.1 *XRD characterization*

The XRD patterns from ZSM-5/11 and Ga-Ag-ZSM-5/11(1), (2) and Zn-Cu-ZSM-5/11(1), (2) are shown in Figure 1a. After metals substitution, the diffraction peaks of all samples are the same, indicating that metal incorporation on the catalyst would not cause any noticeable effect on the synthetic zeolite framework. According to previous reports,[36,38] The MFI and MEL crystal structures in the ZSM-5 and ZSM-11 demonstrated five and two distinct picks in 2θ = 20–25° respectively. It is observed that the intensity of (051) and (303) reflection, in 2θ = 23.2°, 23.6° decrease, and (133) refection in 2θ = 24.4° completely disappears which is a key feature of creation an intergrowth structure between ZSM-5 and ZSM-11 zeolites (Figure 1b).[39]

However, with regard to diffraction at 2θ = 23° it can be seen that the peak intensity has been reduced compared to ZSM-5/11 in metals modified zeolites especially after more loaded metals content (Zn-Cu-ZSM-5/11(2), Ga-Ag-ZSM-5/11(2)) and this reduction in crystallite can occur due to higher absorption coefficient of loading metals or adding of metals during synthesis and the serious dealumination (Table 1).[40,41] Conforming to Debye–Scherer equation, the crystallite size of modified ZSM-5/11 zeolites, has been reduced, which are presented in Table 1. It should be noted that the peak generated at 2θ = 26.6°, which is observed in some spectra, is related to quartz structure. Although unstable phases

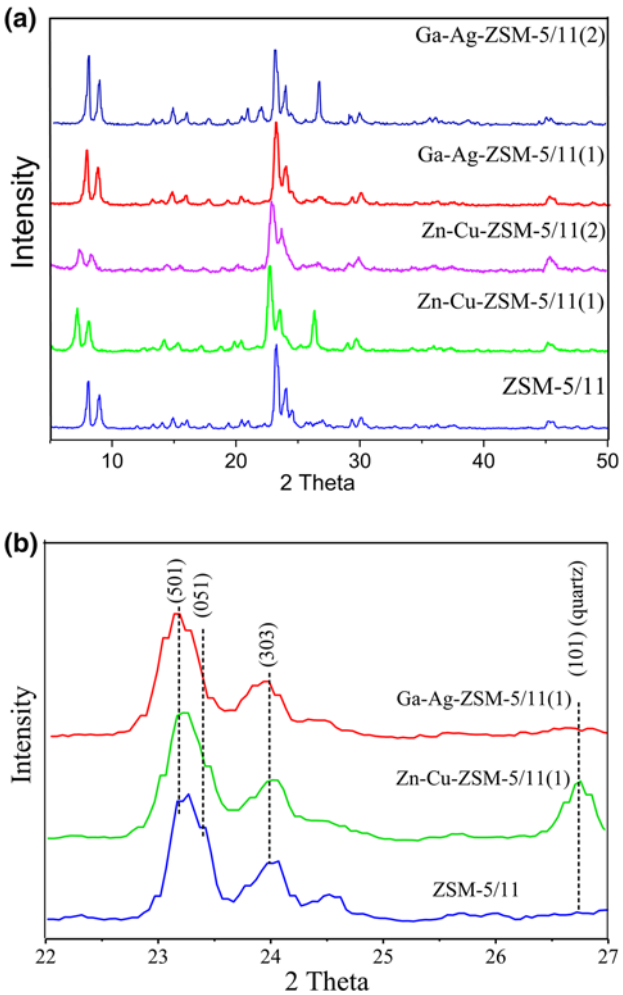

Figure 1. XRD patterns of samples from (a): 2θ = 5° to 50°, (b): 2θ = 22° to 27°.

are destroyed during the crystallization process, quartz with a more stable phase would remain.[36]

3.2 *Electron microscope images*

To evaluate the morphology and dispersion of metal species on zeolites, SEM and TEM micrographs were obtained (Figures 2, 3). SEM images obtained from the ZSM-5/11 sample illustrate that nanocrystalline particles have been synthesized. These particles accumulated in spherical structures and created microparticles. But after substituted metal species, both zeolite samples contain polycrystalline particles in the form of accumulated spherical or cubic with the size of 50–100 nm. The difference in zeolites morphology demonstrated that added metals in the synthesis gel would interact with TBA^+ as an organic template, affecting the structure of zeolite.[42] It is specified that the addition of metals during zeolite synthesis led to smaller crystal size, due to the role of metal species in increasing nucleation during the crystallization process.[43]

Also, SEM images of samples with different content of loaded metals show that with increasing metal loading, there is no change in the structure of the zeolite, although in the Zn-Cu loading sample, the size of crystals is smaller and the surfaces of the particles become flat and uniform.

TEM images show that the rectangular crystals are formed after loading of the metals. Also, metals are uniformly located into the framework of zeolite rather than disperse on the external surface. Although elemental analysis proves that the metal is present in these zeolites, no cumulative metals or metals oxide structure is found in these samples.

3.3 *BET analysis*

In order to study the porosity properties, ZSM-5/11 and metals substitution zeolite samples were investigated with N_2 adsorption-desorption analysis. The texture features obtained from catalysts are shown in Table 2. It is observed that contrary to other methods of loading the metal, which reduced the special surface area and the microporous volume due to the inappropriate distribution of particles and the formation of other phases such as (Ga_2O_3 or ZnO) extra crystalline and blocking of the pores, the direct synthesis method increases the surface area and volume of the pores but average diameters of particles decreases (Table 2).[44] This may have occurred due to the good distribution of metal species or structural defects during catalyst modification.[45]

Comparison of different concentrations of metals for loading into the zeolites by BET analysis indicates that with increasing metals content into the zeolites, the BET surface area and the pores volume are reduced. In these samples, a large amount of metal particles enter into the channels and pores, aggregate and deposit which cause to blockage of the pores of zeolites. Also, agglomeration of some metal particles on the outer surface of zeolite can cause similar effects.[46,47]

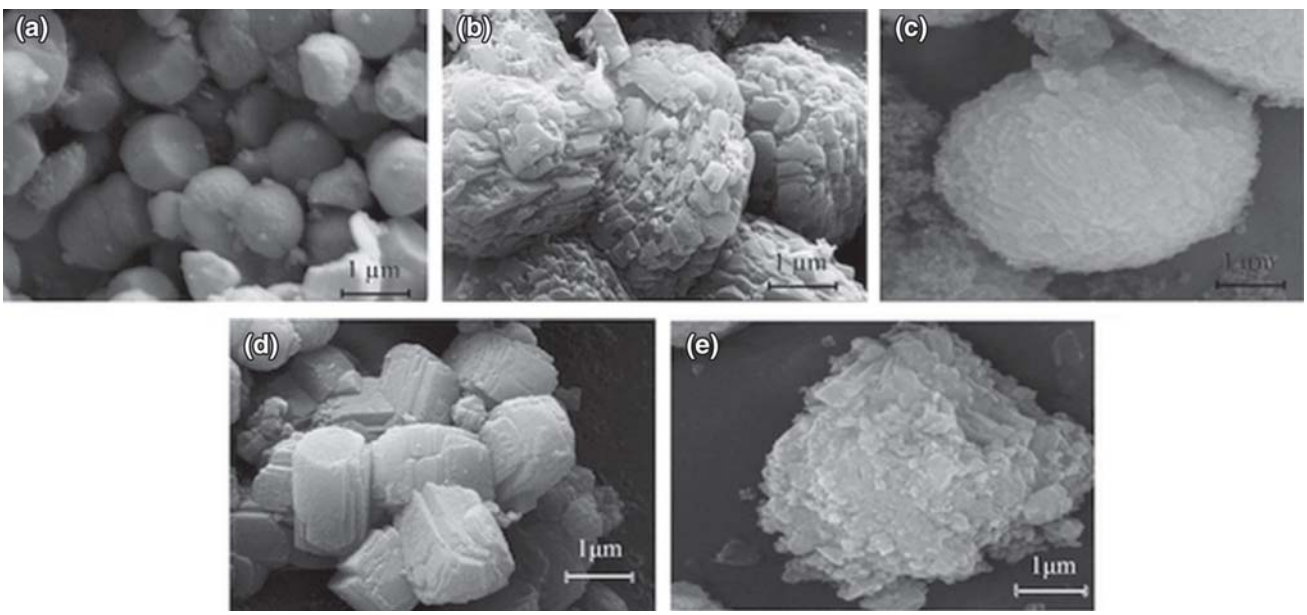

Figure 2. FE-SEM of all samples (a) ZSM-5/11, (b) Zn-Cu-ZSM-5/11(1), (c) Ga-Ag-ZSM-5/11(1), (d) Zn-Cu-ZSM-5/11(2) and (e) Ga-Ag-ZSM-5/11(2).

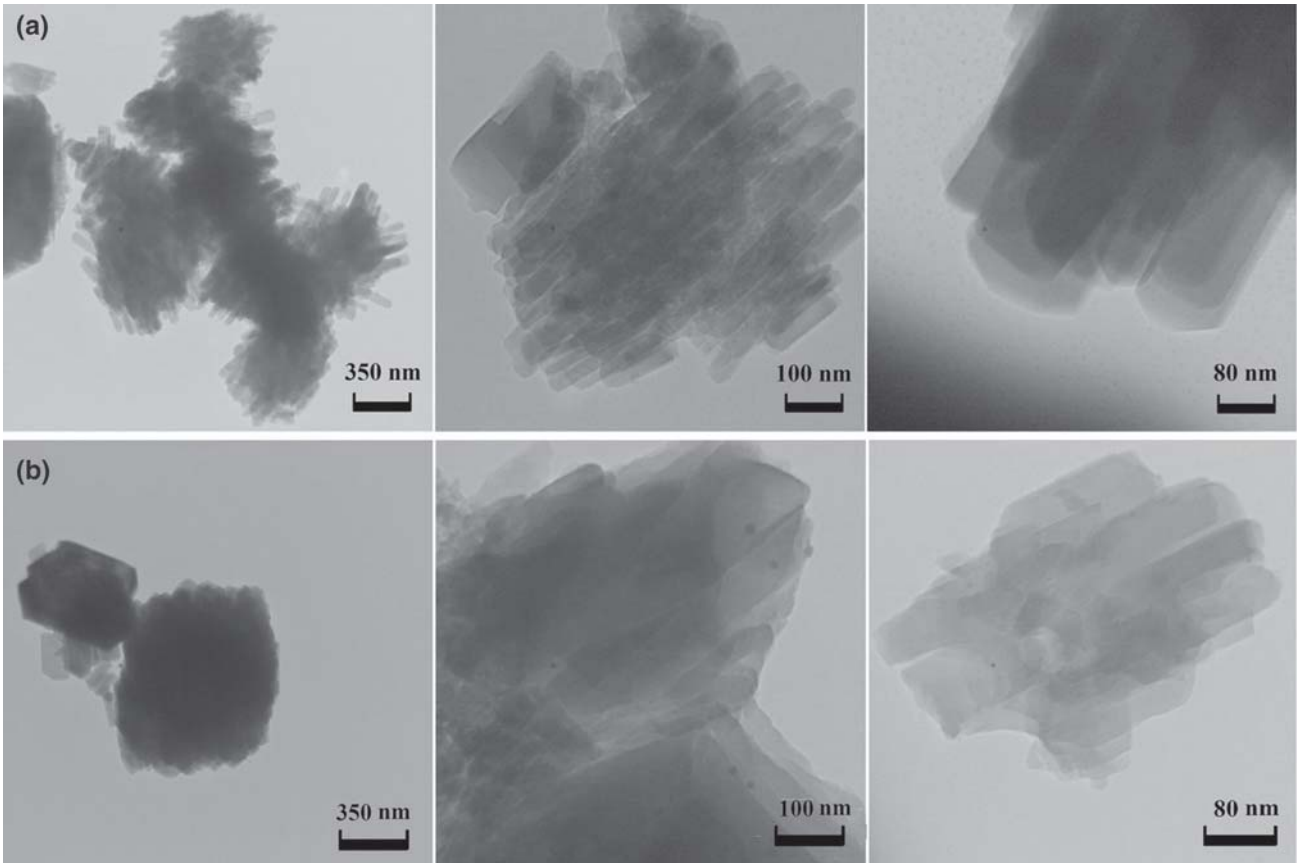

Figure 3. TEM images of (a) Zn-Cu-ZSM-5/11(1), (b) Ga-Ag-ZSM-5/11(1) zeolites with different magnifications.

Table 2. The textural properties of prepared ZSM-5/11 and modified ZSM-5/11.

Sample	S_{BET} (M^2/g)[a]	V_{micro} (cm^3/g)[b]	V_{meso} (cm^3/g)[c]	V_{total} (cm^3/g)[d]	$D_{average}$ (nm)
ZSM-5/11	253.36	0.0582	0.1425	0.2007	3.16
Zn-Cu-ZSM-5/11(1)	353.46	0.0810	0.1606	0.2416	2.51
Zn-Cu-ZSM-5/11(2)	276.64	0.0835	0.1508	0.2343	3.38
Ga-Ag-ZSM-5/11(1)	378.56	0.0869	0.1820	0.2693	2.64
Ga-Ag-ZSM-5/11(2)	291.21	0.0669	0.1469	0.2138	2.92

[a]specific surface area measured by BET analysis.
[b]measured by t-plot method.
[c]$V_{meso} = V_{ads,\ p/po=0.99} - V_{micro}$.
[d]Determined at $p/p_0 = 0.995$.

According to Figure 2(a), the N_2 adsorption-desorption isotherms of all samples exhibit an incremental slope in lower relative pressures which could be attributed to the typed I isotherm with H_4-shaped hysteresis loops indicating the presence of micropores in the structure of zeolites. But at pressures of $0.45 < p/p0 < 0.9$, the hysteresis loops of the modified samples are more distinct than ZSM-5/11 zeolite, indicating mesoporosity increases after incorporation of metals. This phenomenon can be due to the longer M-O (M = Ga, Ag, Zn, Cu) bond and the formation of defects in the zeolites framework. Also, the accumulation of nanoparticles creates an intergranular mesoporous structure in accordance with FE-SEM micrographs.[44] From the pore size distribution curve by the Barrett-Joyner-Halenda (BJH) method, a narrow distribution is observed at about 2–3 nm (Figure 4b). Based on the obtained diagram, after metals

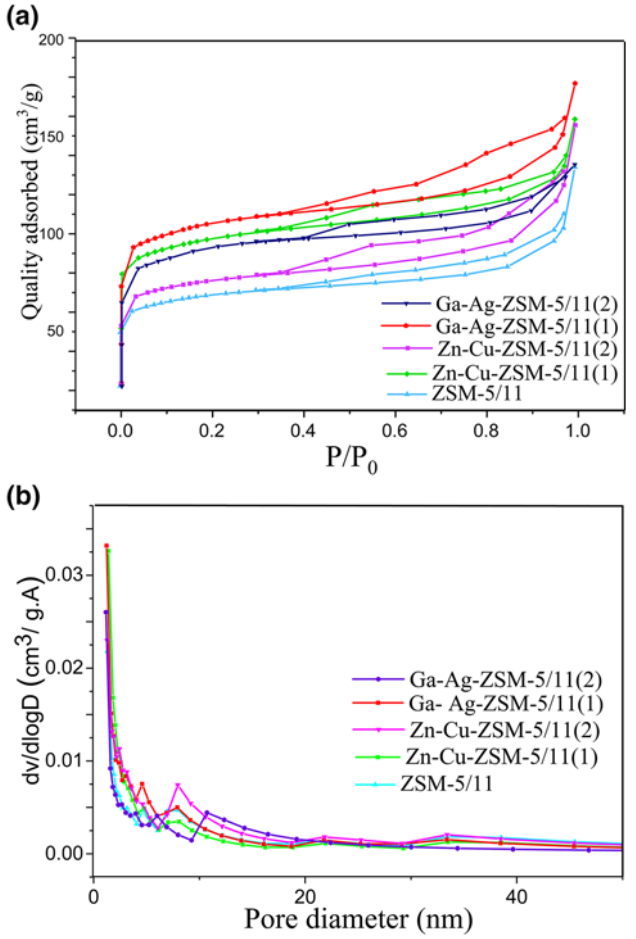

Figure 4. (a) N_2 adsorption-desorption isotherms and (b) BJH pore size distribution of samples.

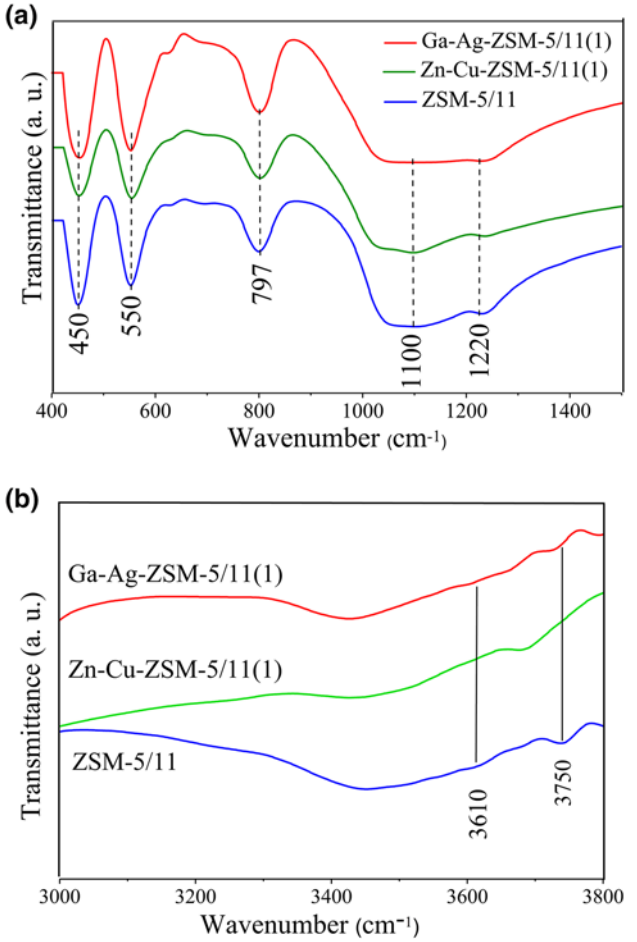

Figure 5. FTIR spectra of prepared samples in the range of (a) 400–1500 cm^{-1} and (b) 3000–3800 cm^{-1}.

incorporation, the pore diameter is not changed significantly.

3.4 *FTIR analysis*

Figure 5 represents infrared spectra of the ZSM-5/11 and after loadings Zn-Cu and Ga-Ag into the catalyst in the range of 400−4000 cm^{-1}. Regarding the FTIR patterns, the spectrum of all samples after metals incorporation is similar to the ZSM-5/11 and demonstrate common characteristic absorption bands at around 450, 550, 797, 1100 and 1225 cm^{-1} regions.[48] The peak at 450 cm^{-1} is related to the vibration of Al (or Si) T-O bond of AlO_4 and SiO_4 in a tetrahedral network. The band at 550 cm^{-1} is correlated with the presence of double five rings which are the characteristic structure of pentasil in MFI and MEL zeolite family.[15] The IR bands 550/450 cm^{-1} ratio (I550/I450) is an approximate estimate of crystalline degree. This ratio decreases slightly after zeolite modification, which is also consistent with the results of XRD.[49] Other bands at 797, 1100 and 1225 cm^{-1} are related to the internal and external asymmetric stretch and external symmetric stretching of Si–O–T linkage in ZSM5/11, respectively. A sharp peak at 1100 cm^{-1} is relevant to the disappearance of surface [O_3Si–OH] units due to a significant reduction in the particle size of zeolites and formation of nanocrystals.[15]

Based on Figure 5(b) in the range of 3500–3800 cm^{-1}, OH-stretch vibrations are observed at 3610 and 3750 cm^{-1}. The band at 3610 cm^{-1} is attributed to the Brønsted acid sites formed by the bridging hydroxyl group located between Si and Al atoms in the zeolite framework.[50] Another O–H band at about 3750 cm^{-1} has been ascribed extra framework isolated silanol groups in inside and outside of zeolites.[51] After incorporation of metal species, intensities of the O–H bands at 3610 cm^{-1} have been reduced, indicating that the metals on the surface and the inner of pores and channels reacted with OH groups and the acidity density has been reduced.[51] These results confirm the data obtained from NH_3-TPD.

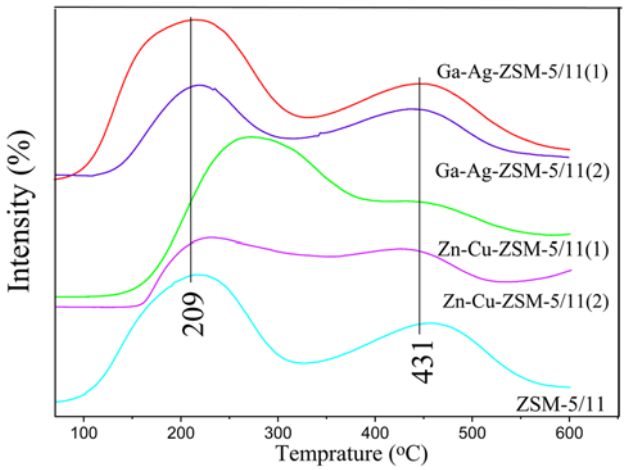

Figure 6. NH_3-TPD profiles of samples.

3.5 *NH_3-TPD analysis*

The NH_3-TPD profile of the ZSM-5/11 catalyst and after metals incorporation has been performed. The results shown in Figure 6 are for comparison of changes in the concentration and strength of the acidity catalyst. For all the samples, two distinct peaks appear in a temperature range of 200–300 °C and 400–600 °C assigned to NH_3 desorption from weak (Lewis) and strong (Brønsted) acid sites, respectively. Also calculated amount of weak, strong and total acid sites have been presented in Table 3.

Based on the NH_3-TPD results, it is clear that the weak acidity (Lewis) peak shifts toward high temperatures with increasing intensity, compared to ZSM-5/11, indicates new moderate Lewis acid sites are formed.

After introducing metal species M (Zn, Cu, Ga, Ag) into the zeolite framework, they can react with acidic OH groups and produce M-OH $^{+}$. This M-OH^{+} species contain a higher electron-accepting ability and show a strong interaction with the negative charge generated by the internal silanol groups. According to the following reaction, the M-O-Si bonds are formed as the new moderate Lewis acid sites.

$$\text{ZO-MOH}^{+} + \text{Si-OH} \rightarrow \text{ZO-M-O-Si}$$

The new M-Lewis acid sites improve the alkenes dehydrogenation process to aromatics. These sites are more selective to aromatic products, especially BTX, and by controlling the hydrogen transfer reaction, they slow down the formation of heavy aromatics, resulting in a better anti-coking capacity than the Brønsted acidic centers.[26]

As the previous studies, the strong acidity in Gallium-containing samples has been increased significantly. It was due to the formation of extra-framework GaO^{+} species into the framework. It has also been cleared that the direct synthesis method for Ga loading increased the formation of GaO^{+} species with stronger acid sites.[44] But after substituting both Ga and Ag metals, it seems that some acid sites, in addition to Ga species, interact with Ag species, and the intensity of the Lewis and Brønsted acidic centers is lower than the gallium-containing sample which can be moderated formation of aromatic products. According to our studies and other reports, adding second metal has a greater effect on the reduction of acidity, especially on the Brønsted acid sites.[30,32]

In addition, the results of NH_3-TPD in Table 3 show that by increasing the loading of metals, the concentrations of Lewis and Brønsted acid, and consequently the total acidity, decreased due to the excessive accumulation of metal species on the external surface of zeolite and inside the pores, which produced a negative effect on increased acidity sites.[46]

3.6 *Catalytic performance test*

Catalytic conversion of methanol was investigated with time on stream (TOS) over the prepared catalysts, at 390 °C, WHSV of 4.7 h^{-1} and atmospheric

Table 3. NH_3 –TPD data of prepared ZSM-5/11 and modified ZSM-5/11.

Sample	Peak temperature (°C)		Acidity (mmol/g)		
	T_{P1}	T_{P2}	Weak	Strong	Total
ZSM-5/11	209	431	0.81	0.64	1.45
Zn-Cu-ZSM-5/11(1)	315	635	1.34	0.56	1.90
Zn-Cu-ZSM-5/11(2)	260	473	0.49	0.55	1.04
Ga-Ag-ZSM-5/11(1)	214	458	1.04	0.79	1.84
Ga-Ag-ZSM-5/11(2)	241	413	0.36	0.36	0.72

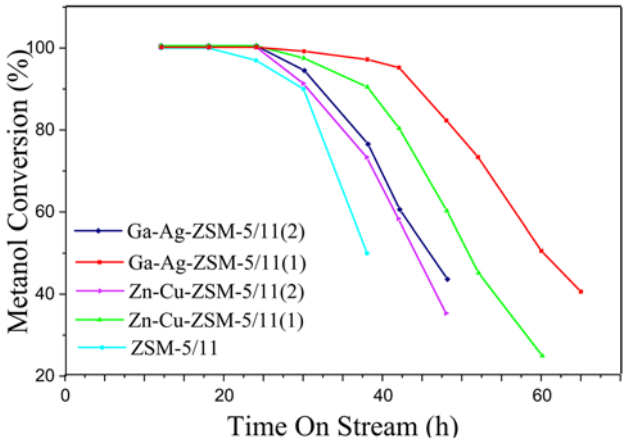

Figure 7. Methanol conversion with the time-on-stream (TOS) over the prepared zeolites (Reaction conditions: T = 390 °C, P = 1 atm, WHSV = 4.5 h^{-1}).

pressure. Based on Figure 7, with ZSM-5/11 catalyst, methanol conversion is about 100% after 20 h on stream then decrease sharply. But after incorporation of metals, it is observed that conversion of methanol with Zn-Cu-ZSM-5/11(1) and Ga-Ag-ZSM-5/11(1) catalysts remain about 90% during the 38 and 42 h respectively, then a slower drop is observed for these catalysts, due to the reduced crystallite size according to the result of XRD and SEM analysis and increased in mesopore volume and intercrystalline porosity based on the BET and SEM data. This improvement in catalysts structure reduces the length of products pathway in channels and pores that prevent the formation of coke and catalyst deactivation.

It is also indicated that with increasing the amount of incorporated metals, the lifetime of the catalyst is reduced to 30 h, which can be due to the increased mesopore volume, reduced BET surface area and the acidic site's density, according to spectroscopic studies.

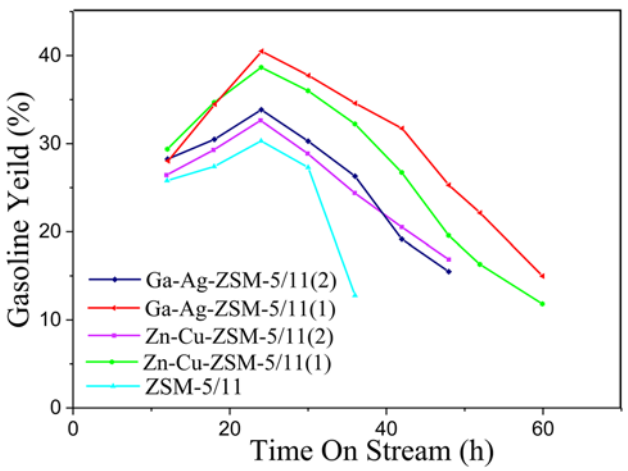

Figure 8. Gasoline yield with the time-on-stream (TOS) over the prepared zeolites (Reaction conditions: T = 390 °C, P = 1 atm, WHSV = 4.5 h^{-1}).

Gasoline products that only contain liquid hydrocarbons, collected at different times during the MTA process, have been represented in Figure 8. The highest amount of produced gasoline by ZSM-5/11 zeolite is about 30.3 wt%, which was generated in 24 h on stream and immediately declines to 12.78 wt% within 24 to 36 h. However, the production amount is increased to 38.7 wt% and 40.4 wt% with Zn-Cu-ZSM-5/11(1) and Ga-Ag-ZSM-5/11(1) catalysts, in the same time (24 h), respectively. Over time, hydrocarbon products, especially aromatics, inside the zeolite pores undergo successive reactions through the carbon pool mechanism, including methylation of aromatics, and the formation of char and polyaromatic precursors as coke. Accumulation of coke deposits inside the zeolite cage cause blocking the zeolite inner pores and prevent the penetration of other reactants and products. The produced hydrocarbons cannot easily be transported to the external surface, causing the acidic sites to be inaccessible inside the pores, thereby the production of hydrocarbon products and the stability of the catalyst during the reaction time have been reduced.[52]

After loading the metals, based on the XRD and BET results, the size of the crystalline particles decreases and the intercrystalline porosity and BET surface area increase. On the other hand, according to the results of FTIR and NH_3-TPD, the acidity and extra framework isolated silanol groups inside and outside of zeolites reduce. These changes lead to the production of gasoline range hydrocarbons continue for longer periods of time and contrary to the ZSM-5/11 sample, the gasoline production during the reaction is not rapidly reduced.

However, in the samples with higher metal content (Zn-Cu-ZSM-5/11(2) and Ga-Ag-ZSM-5/11(2)), the amount of hydrocarbon production is reduced to 31.8 wt% and 32.1 wt% due to the blockage of the internal pores and channels and the lack of access to acidic sites, and as a result they are also deactivated more quickly.

Results of gas chromatography and the distribution of the products are represented in Table 4. It can be seen that aromatic products predominate over other constituents of gasoline. First, intergrowth structure between ZSM-5 and ZSM-11 zeolites leads to shape the selectivity and the relative increase in the size of cross-channel in this structure which have a great impact on the production of hydrocarbon products, especially high aromatics content (84.52 wt% with

Table 4. The liquid hydrocarbon distribution over prepared catalysts.

Compound	ZSM-5/11	Zn-Cu-ZSM-5/11(1)	Zn-Cu-ZSM-5/11(2)	Ga-Ag-ZSM-5/11(1)	Ga-Ag-ZSM-5/11(2)
Liquid hydrocarbons Yield %	30.30	38.7	31.8	40.4	32.1
Product distribution (%)					
Paraffins	0.33	3.70	7.65	7.40	6.36
Cycloparaffins	3.97	4.86	7.56	6.06	7.71
Alkenes	2.87	4.14	2.91	5.39	5.69
Cycloalkenes	5.65	6.17	5.47	9.84	12.43
Others	3.25	1.27	1.6	2.32	2.09
Total Aromatics	84.52	79.86	74.81	67.76	65.43
Aromatics distribution (%)					
Benzene	1.98	2.29	1.73	1.72	1.72
Toluene	1	4.34	3.28	2.99	2.97
o- Xylene	–	–	–	–	–
P-Xylene	21.52	14.10	17.13	15.19	12.83
m-Xylene	–	9.70	–	5.9	4.42
Ethyl-Benzene	1.98	0.92	1.47	2.0	1.42
C_9	29.62	29.79	24.30	22.62	23.05
C_{10}	13.90	8.58	11.80	6.50	7.43
C_{10}^+	16.66	11.04	16.41	13.74	13.06

ZSM-5/11). But, this catalyst is not stable and is quickly deactivated (Figure 7).

Based on Table 4 it seems that the total amount of aromatic compounds is reduced to 79.86 wt% and 67.76 wt% respectively using Zn-Cu-ZSM-5/11(1), Ga-Ag-ZSM-5/11(1), relative to 84.52 wt% with ZSM-5/11 sample. The reduction of acidic sites and the size of crystalline particles and the increase of mesopore volume in metal incorporated samples can be a reason to reduce the amount of aromatics. The Brønsted acid sites are active centers for secondary reactions such as polymerization and hydride transfer on olefins, which results in the formation of aromatic compounds.

In our review, based on the NH_3-TPD and Table 3 data, the amount of Brønsted acidity decreased in the Zn-Cu-ZSM-5/11 sample compared with ZSM-5/11. In the case of Ga-Ag-ZSM-5/11, the acidity sites have increased, due to the presence of extra-framework GaO^+ species. But the amount of aromatic production with the desired catalysts changes as follows.

$$\text{H - ZSM - 5/11(84.52)} > \text{Zn - Cu - ZSM} - 5/11\,(79.86) > \text{Ga - Ag - ZSM} - 5/11(67.76)$$

This shows that the amount of acidic sites is not only an effective factor in aromatics production, but the pores structure and crystalline size are also involved. Reducing the crystalline size along with the mesopore volume can shorten the length of the penetration pathway in the pores of metals loading zeolites, and the reactants can easily be removed from the pores and channels prior to further and sequential reactions that lead to formation the heavier hydrocarbons. Thus, the production of the aromatic reduces in the metal substituted samples than ZSM-5/11. In ZSM-5/11, the primary aromatics include benzene, toluene, xylene (BTX), in the pores under subsequent reactions, convert to heavy hydrocarbons and their amounts are reduced. But in metal incorporated zeolites, BTX compounds after production remove from the channels

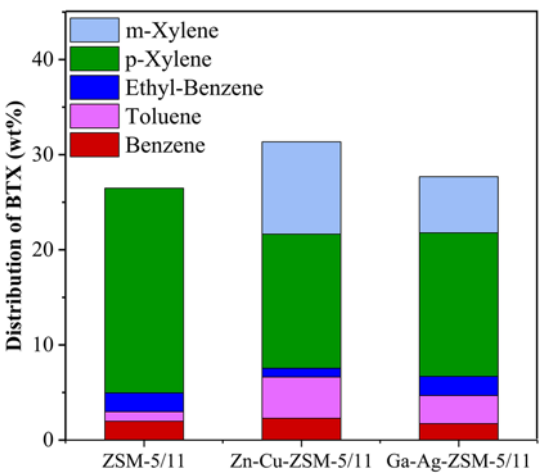

Figure 9. Distribution of BTX in MTA process (Reaction conditions: T = 390 °C, P = 1 atm, WHSV = 4.5 h^{-1}).

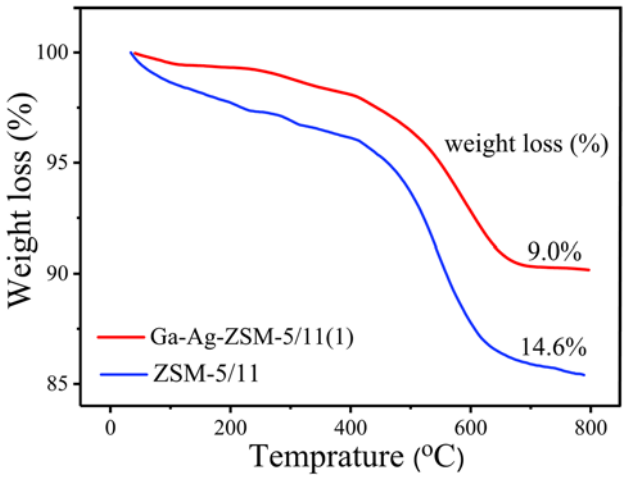

Figure 10. TGA analysis of coke content on ZSM-5/11 and Ga-Ag-ZSM-5/11.

and the pores mouth before the secondary reactions. Consequently, their amount increases among the total aromatic products.

Also, the reduction of aromatics is accompanied by an increase in the production of paraffins and cycle-paraffins, which is related to the reduction of crystalline dimensions. In smaller crystalline zeolites, due to the high surface area and the outer surface acidic sites, most disproportionation and isomerization reactions on hydrocarbons occur at the outer surfaces, leading to more paraffin's formation.

Chen *et al.,* investigated the catalytic aromatization of CH_3Br with HZSM-5, CuO/HZSM-5, ZnO/HZSM-5 and CuO-ZnO/HZSM-5 catalysts. They observed CuO/HZSM-5 and CuO-ZnO/HZSM-5 had both strong and weak acid sites according to the NH_3-TPD. Furthermore, they had a higher selectivity to heavy aromatics C $\geq$ 10. On the other hand, in HZSM-5 and ZnO/HZSM-5 catalysts acid sites were weak and aromatic hydrocarbons lighter than C_6-C_8 produced with these catalysts.[53]

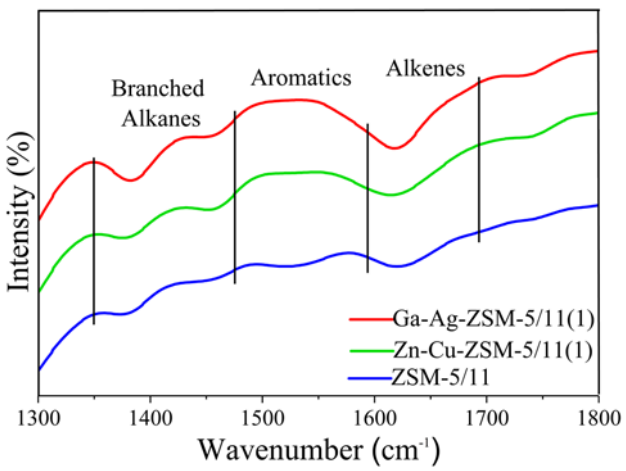

Figure 11. FT-IR spectra of coked catalysts in the range of 1300–1800 cm^{-1}.

The last but not the least, the catalyst substitution method also has a significant effect on the yield and the lifetime of a catalyst.[43] It became clear that the direct synthesis method is an effective method for loading of metals in the structure of zeolite and lets to uniform distribution of metals particles according to the TEM in Figure 4 (metal species are not observed in the images). This appropriate distribution of metals particles causes the formation of the new and moderate acidity. As mentioned before, this acidity is suitable for the formation of aromatic compounds, especially BTX, and resulting in a more stable catalyst in the MTA process (Figure 9). Yang and colleagues also proved that, the addition of Sn-metal into the ZSM-5 zeolite framework with the direct synthesis method induced the uniform distribution of the particles and amended BTX production.[54]

In the following, the coked ZSM-5/11 and Ga-Ag-ZSM-5/11(1) catalysts were analyzed after MTA reaction with the thermogravimetric method (TGA) under flowing air. Figure 10 displays the TGA curves of the used catalysts. Distinctive catalyst weight loss in a temperature range of 300–700 °C is related to the coke amount. The rate of coke formation is determined as lost weight divided by the catalyst lifetime (h).[55] According to this result, the average rate of coke formation on the ZSM-5/11 catalyst is about 0.4% per hour, but after metals incorporation into the catalyst, this amount is reduced to 0.14 per hour. Low amount of coke formation has been explained by the formation of the new moderate acid sites, increased intercrystalline porosity and reduced crystalline size of the particles in Ga-Ag-ZSM-5/11(1) compared with ZSM-5/11.

Also, IR spectroscopy technique was used to investigate the nature of coke species generated in the channels and pores of the catalysts during the methanol conversion process. The spectra of the catalysts were obtained after reaction (Figure 11). As reported by previous studies,[56] the peaks in the region of 1350–1470 cm^{-1}, around 1600 cm^{-1} and 1600–1700 cm^{-1} associate with branched alkanes, aromatics and poly-alkaline structures and alkenes forming in catalysts respectively. In the Figure 11, it is observed that with ZSM-5/11 catalyst, a small band in 1470–1600 cm^{-1} can be seen that is due to the formation of heavy aromatic species as deposited coke within this zeolite. But after modification, produced hydrocarbons, particularly aromatics, have not yet occupied channels and pores. Also, it is observed that

the amount of alkenes and Alkanes are increased over Ga-Ag substitution catalysts which is in accordance with the GC-MS results.

4. Conclusions

Nano-crystalline ZSM-5/11 was successfully synthesized by hydrothermal method, and direct synthesis procedure was used for loading Zn-Cu and Ga-Ag species into the framework of ZSM-5/11 with different content. The obtained results showed that after substitution metal species, crystal size and average diameters of particles decreased, while the surface area and pore volume increased. The NH_3-TPD results implied that the incorporated Cu-Zn replaced parts of the conventional acid sites and formed some new acid sites in the zeolites. This new acid sites significantly improved the hydrogen transfer and aromatization reaction, increasing the yield of production. Also, the results of NH_3-TPD showed that the effect of loading Ag with Ga in bimetallic Ga-Ag-ZSM-5/11 caused an adjustment in the amount of acid sites. Ag particles react with some of Lewis and Brønsted acidic centers and create new Ag-Lewis acidity sites. This new acidity sites, with moderated strength, can improve the formation of the desired aromatics, especially BTX, and decrease the formation of heavy aromatics. Also, it became clear that the stability of low metal content zeolites (Zn-Cu-ZSM-5/11(1) and Ga-Ag-ZSM-5/11(1)) with mesopore structure and moderated acidity sites compared to ZSM-5/11 increased from 24 h to 38 and 42 h respectively.

Acknowledgements

The second author of this paper gratefully acknowledges the support from Department of Food Science and Agricultural Chemistry, Macdonald Campus, McGill University and special thanks to Dr. Ashraf Ismail for providing research facilities.

References

1. Tian-cai H, Xiao-han C, Ling L and Guo-ying M 2009 Study of methanol-to-gasoline process for production of gasoline from coal *J. Coal. Sci. Eng*. **15** 104
2. Ni Y, Sun A, Wu X, Hai G, Hu J, Li T and Li G 2011 The preparation of nano-sized H[Zn, Al]ZSM-5 zeolite and its application in the aromatization of methanol *Micropor. Mesopor. Mater*. **143** 435
3. Wei Z, Chen L, Cao Q, Wen Z, Zhou Z, Xu Y and Zhu X 2017 Steamed Zn/ZSM-5 catalysts for improved methanol aromatization with high stability *Fuel. Process. Tech*. **162** 66
4. Hu H, Cao F, Ying W, Sun Q, Fang D 2010 Study of coke behavior of catalyst during methanol-to-olefins process based on a special TGA reactor *Chem. Eng. J.* **160** 770
5. Aramburo L R, Teketel S, Svelle S, Bare S R, Arstad B, Zandbergen H W, Olsbye U, Groot F and Weckhuysen B M 2013 Interplay between nanoscale reactivity and bulk performance of H-ZSM-5 catalysts during the methanol-to-hydrocarbons reaction *J. Catal.* **307** 185
6. Li J, Wang Y, Jia W, Xi Z, Chen H, Zhu Z and Hu Z 2014 Effect of external surface of HZSM-5 zeolite on product distribution in the conversion of methanol to hydrocarbons *J. Energy Chem.* **23** 771
7. Saxena S K, Viswanadham N and Al-Muhtase A H 2014 Enhanced production of high octane gasoline blending stock from methanol with improved catalyst life on nano-crystalline ZSM-5 catalyst *J. Ind. Eng. Chem.* **20** 2876
8. Boukoussa B, Aouad N, Hamacha R and Bengueddach A 2015 Key factor affecting the structural and textural properties of ZSM-5/MCM-41 composite *J. Phys. Chem. Solids* **78** 78
9. Wang B, Tian Z, Li P, Wang L, Xu Y, Qu W, Ma H, Xu Z and Lin L 2009 Synthesis of ZSM-23/ZSM-22 intergrowth zeolite with a novel dual-template strategy *Mater. Res. Bull.* **44** 2258
10. Di Z, Yang C, Jiao X, Li J, Wua J and Zhang D 2013 A ZSM-5/MCM-48 based catalyst for methanol to gasoline conversion *Fuel* **104** 878
11. Jablonski G A, Sand L B and Gard J A 1986 Synthesis and identification of ZSM-5/ ZSM-11 pentasil intergrowth structures *Zeolites* **6** 396
12. Wang X, Chen H, Meng F, Gao F, Sun C, Sun L, Wang S, Wang L and Wang Y 2017 CTAB resulted direct synthesis and properties of hierarchical ZSM-11/5 composite zeolite in the absence of template *Micropor. Mesopor. Mater.* **243** 271
13. Francesconi M S, López E, Tegui D U, González G, Hernández J C, Uzcátegui A, Loaiza A and Imbert F E 2005 MFI/MEL intergrowth and its effect on n-decane cracking *Catal. Today*. **107** 809
14. Yu Q, Chen J, Zhang Q, Li C and Cui Q, 2014 Micron ZSM-11 microspheres seed-assisted synthesis of hierarchical submicron ZSM-11 with intergrowth morphology *Mater. Lett*. **120** 97
15. Yu Q, Cui C, Zhang Q, Chen J, Li Y, Sun J, Li C, Cui Q, Yang C and Shan H 2013 Hierarchical ZSM-11 with intergrowth structures: Synthesis, characterization and catalytic properties *J. Energy Chem*. **22** 761
16. Li P, Zhang W, Han X and Bao X 2010 Conversion of Methanol to Hydrocarbons over Phosphorus-modified ZSM-5/ZSM-11 Intergrowth Zeolites *Catal. Lett*. **134** 124
17. Jiang X, Su X, Bai X, Li Y, Yang L, Zhang K, Zhang Y, Liu Y and Wu W 2018 Conversion of methanol to light olefins over nanosized [Fe,Al]ZSM-5 zeolites: Influence of Fe incorporated into the framework on the acidity and catalytic performance *Micropor. Mesopor. Mater*. **263** 243
18. Liu S, Gujar A C, Thomas P, Toghiani H and White M G 2009 Synthesis of gasoline-range hydrocarbons over Mo/HZSM-5 catalysts *Appl. Catal. A* **357** 18

19. Jiang S, Zhang H and Yan Y 2018 Cu-MFI zeolite supported on paper-like sintered stainless fiber for catalytic wet peroxide oxidation of phenol in a batch reactor *Sep. Pur. Tech.* **190** 243
20. Hu H, Zhang Q, Cen J and Li X 2014 High suppression of the formation of ethylbenzene in benzene alkylation with methanol over ZSM-5 catalyst modified by platinum *Catal. Commun.* **57** 129
21. Kim S, Park G, Kim S K, Kim Y T, Jun K and Kwak G 2018 Gd/HZSM-5 catalyst for conversion of methanol to hydrocarbons: Effects of amounts of the Gd loading and catalyst preparation method *Appl. Catal. B* **220** 191
22. Stepacheva A A, Doluda V Y, Lakina N V, Molchanov V P, Sidorov A I, Matveeva V G, Sulman M G and Sulman E M 2018 Catalytic performance of the modified H-ZSM-5 zeolite in methanol transformation to hydrocarbons *React. Kinet. Mech. Cat.* **124** 823
23. Song C, Li X, Zhu X, Liu S, Chen F, Liu F and Xu L 2016 Influence of the state of Zn species over Zn-ZSM-5/ZSM-11 on the coupling effects of cofeeding n-butane with methanol *Appl. Catal. A* **519** 48
24. Li M, Zhou Y, Oduro I N and Fang Y 2015 Comparative study on the catalytic conversion of methanol and propanal over Ga/ZSM-5 *Fuel* **168** 68
25. Sun L, Guo X, Liu M and Wang X 2009 Ethylation of coking benzene over nanoscale HZSM-5 zeolites: Effects of hydrothermal treatment, calcination and La_2O_3 modification *Appl. Catal. A* **355** 184
26. Niu X, Gao J, Wang K, Miao Q, Dong M, Wang G, Fana W, Qin Z and Wang J 2017 Influence of crystal size on the catalytic performance of H-ZSM-5 and Zn/H-ZSM-5 in the conversion of methanol to aromatics *Fuel. Process. Tech.* **157** 99
27. Borght K V, Galvita V V and Marin G B 2015 Reprint of "Ethanol to higher hydrocarbons over Ni, Ga, Fe-modifiedZSM-5: Effect of metal content *Appl. Catal. A* **504** 621
28. Mentzela U V, Højholt K T, Holm M S, Fehrmann R and Beatoc P 2012 Conversion of methanol to hydrocarbons over conventional and mesoporous H-ZSM-5 and H-Ga-MFI: Major differences in deactivation behavior *Appl. Catal. A* **417** 290
29. Tshabalala T E and Scurrell M S 2015 Aromatization of n-hexane over Ga, Mo and Zn modified H-ZSM-5 zeolite catalysts *Catal. Commun*. **72** 49
30. Oliveira1 T K R, Rosset1 M and Perez-Lopez O W 2018 Ethanol dehydration to diethyl ether over Cu-Fe/ZSM-5 catalysts *Catal. Commun*. **104** 32
31. Youming N, Aiming S, Xiaoling W, Jianglin H, Tao L and Guangxing L 2011 Aromatization of Methanol over La/Zn/HZSM-5 Catalysts *Chin. J. Chem. Eng*. **19** 439
32. Majhi S and Pant K K 2014 Direct conversion of methane with methanol toward higher hydrocarbon over Ga modified Mo/H-ZSM-5 catalyst *J. Ind. Eng. Chem*. **20** 2364
33. Li X, Shen B and Xu C 2010 Interaction of titanium and iron oxide with ZSM-5 to tune the catalytic cracking of hydrocarbons *Appl. Catal. A* **375** 222
34. He P, Gatip R, Yung M, Zeng H and Song H 2017 Co-Aromatization of Olefin and Methane over Ag-Ga/ZSM-5 Catalyst at Low Temperature *Appl. Catal. B* **211** 275
35. Zaidi H A and Pant K K 2004 Catalytic conversion of methanol to gasoline range hydrocarbons *Catal. Today* **96** 155
36. Conte M, Xu B, Davies T E, Bartley J K, Carley A F, Taylor S H, Khalid K and Hutchings G J 2012 Enhanced selectivity to propene in the methanol to hydrocarbons reaction by use of ZSM-5/11 intergrowth zeolite *Micropor. Mesopor. Mater.* **164** 207
37. He P, Luan Y, Zhao L, Cheng W, Wu C, Chen S and Song H 2017 Catalytic bitumen partial upgrading over Ag-Ga/ZSM-5 under methane environment *Fuel Proc. Tech.* **156** 290
38. Li X, Wang C, Liu S, Xin W, Wang Y, Xie S and Xu L 2011 Influences of alkaline treatment on the structure and catalytic performances of ZSM-5/ZSM-11 zeolites with alumina as binder *J. Mol. Catal. A* **336** 34
39. Zhang Y, Zhai X, Zhang H and Zhao J 2017 Enhanced selectivity in the conversion of glycerol to pyridine bases over HZSM-5/11 intergrowth zeolite *RSC Adv*. **7** 23647
40. Zhuang J, Ma D, Yang G, Yan Z, Liu X, Liu X, Han X, Bao X, Xie P and Liu Z 2004 Solid-state MAS NMR studies on the hydrothermal stability of the zeolite catalysts for residual oil selective catalytic cracking *J. Catal.* **228** 234
41. Li J, Miao P, Li Z, He T, Han D, Wu J, Wang Z and Wu J 2015 Hydrothermal synthesis of nanocrystalline H[Fe, Al]ZSM-5 zeolites for conversion of methanol to gasoline *Energy Convers. Manag.* **93** 259
42. Yu Q, Li Y, Meng X, Cui Q and Li C 2014 One-step synthesis of hierarchical Zn-ZSM-11 via a facile ZnO route *Mater. Lett.* **124** 204
43. Niu X, Gao J, Miao Q, Dong M, Wang G, Fan W, Qin Z and Wang J 2014 Influence of preparation method on the performance of Zn-containing HZSM-5 catalysts in methanol-to-aromatics *Micropor. Mesopor. Mater*. **197** 252
44. Fang Y, Su X, Bai X, Wu W, Wang G, Xiao L and Yu A 2017 Aromatization over nanosized Ga-containing ZSM-5 zeolites prepared by different methods: Effect of acidity of active Ga species on the catalytic performance *J. Energy Chem*. **26** 768
45. Yaripour F, Shariatinia Z, Sahebdelfar S and Irandoukht A 2015 Effect of boron incorporation on the structure, products selectivities and lifetime of H-ZSM-5 nanocatalyst designed for application in methanol-to-olefins (MTO) reaction *Micropor. Mesopor. Mater*. **203** 41
46. Li C, Ma J, Xiao Z, Hector S, Liu R, Zuo S, Xie X, Zhang A, Wu H and Liu Q 2018 Catalytic cracking of Swida wilsoniana oil for hydrocarbon biofuel over Cu modified ZSM-5 zeolite *Fuel* **218** 59
47. Zaidi H and Pant K 2005 Catalytic Activity of Copper Oxide Impregnated HZSM-5 in Methanol Conversion to Liquid Hydrocarbons *Can. J. Chem. Eng.* **83** 970
48. Sadeghi S, Haghighi M and Estifaee P 2015 Methanol to clean gasoline over nanostructured CuO-ZnO/HZSM-5 catalyst: Influence of conventional and ultrasound assisted coimpregnation synthesis on catalytic properties and performance *J. Nat. Gas Sci. Eng*. **24** 302

49. Ahmadpour J and Taghizadeh M 2015 Catalytic conversion of methanol to propylene over high-silica mesoporous ZSM-5 zeolites prepared by different combinations of mesogenous templates *J. Nat. Gas Sci. Eng*. **23** 184
50. Barbera K, Bonino F, Bordiga S, Janssens T and Beato P 2011 Structure–deactivation relationship for ZSM-5 catalysts governed by framework defects *J. Catal.* **280** 196
51. Qiu P, Lunsford J and Rosynek M 1998 Characterization of Ga/ZSM-5 for the catalytic aromatization of dilute ethylene streams *Catal. Lett.* **52** 37
52. Kim J, Choi M and Ryoo R 2010 Effect of mesoporosity against the deactivation of MFI zeolite catalyst during the methanol-to-hydrocarbon conversion process *J. Catal.* **269** 219
53. Chen H, Chen T, Chen K, Fu J, Lu X and Ouyang P 2018 Catalytic aromatization of methyl bromide to aromatics over bimetallic CuO-ZnO/HZSM-5 *Catal. Commun.* **103** 38
54. Yang X, Wang F, Wei R, Li S, Wu Y, Shen P, Wang H, Gao L and Xiao G 2018 Synergy effect between hierarchical structured and Sn-modified H[Sn, Al]ZSM-5 zeolites on the catalysts for glycerol aromatization *Micropor. Mesopor. Mater*. **218** 59
55. Noor P, Khanmohammadi M, Roozbehani B, Yaripour F and Garmarudi A B 2018 Introduction of table sugar as a soft second template in ZSM-5 nanocatalyst and its effect on product distribution and catalyst lifetime in methanol to gasoline conversion *J. Energ. Chem*. **27** 582
56. Zhang L, Liu H, Li X, Xie S, Wang Y, Xin W, Liu S and Xu L 2010 Differences between ZSM-5 and ZSM-11 zeolite catalysts in 1-hexene aromatization and isomerization *Fuel. Proc. Tech*. **91** 449